2021 43rd Annual International Conference of the
IEEE Engineering in Medicine & Biology Society (EMBC)
Oct 31 - Nov 4, 2021. Virtual Conference

Evaluation of Patient Positioning to Mitigate RF-induced Heating of Cardiac Implantable Electronic Devices for Pediatric MRI Exams

Jessica A. Martinez, Tyler E. Cork, Henry Chubb, Shreyas Vasanawala and Daniel B. Ennis

Abstract— **Pediatric patients with cardiac implantable electronic devices (CIEDs) are generally contraindicated for MRI exams. Previous work in the adult population suggests that RF-induced lead-tip heating strongly depends on the patient's position and orientation within the MRI scanner. The objective of this work was to evaluate the local Specific Absorption Rate (local-SAR) *in silico* for several pediatric patient positions within the MRI scanner as a method to potentially mitigate RF-heating lead-tip heating of CIEDs.**

I. Introduction

Pediatric patients with complex cardiac disorders are more likely to require cardiac implantable electronic devices (CIEDs) [1], [2] and require a subsequent evaluation and monitoring of multiple organ systems with magnetic resonance imaging (MRI) [3], [4]. The MRI evaluation may include cardiac and non-cardiac imaging since brain, abdominal, and skeletal abnormalities are frequent in pediatrics with CIEDs.

MRI safety analyses of CIEDs have been conventionally performed for transvenous leads. However, CIED with transvenous leads is not possible in pediatric patients owing to their small size. Consequently, epicardial leads are used routinely. Previous work has shown that the presence of epicardial leads raises safety concerns related to RF-induced lead-tip heating (LTH) [5]. Consequently, MRI exams with epicardial CIEDs are broadly contraindicated in the pediatric patient population. Nonetheless, If the clinical benefits of an MRI exam outweigh the risks, then it is necessary to ensure that LTH is minimized.

LTH unavoidably arises as a consequence of the coupling of the RF field with the CIED's leads, which induces electrical energy along the lead and subsequently deposits energy in the cardiac tissue. The amount of energy deposition is measured by the local specific absorption rate (SAR_{local}, W/kg). The magnitude of SAR_{local} and therefore LTH are affected by modifying the incident RF E-field [6]. Thus, LTH can be reduced by simply modifying the pediatric patient's position within the MRI scanner so that their CIED lies within the lowest possible incident E-field. Compared to the adult population, pediatric patients present more degrees of freedom when it comes to body position/orientation within the MRI scanner, owing to their smaller size. In this work, we sought to evaluate *in silico* several pediatric patient-positions and orientations within the MRI scanner as methods to reduce RF-induced LTH.

II. Methods

Numerical simulations were performed using the finite element method (FEM) full-wave electromagnetic solver HFSS (Ansys Inc., Canonsburg, PA) on a 6-year-old pediatric heterogenous human model from the Virtual Family (Thelonious, IT'IS Foundation) with four tissue compartments with different electrical properties (bone, skeletal muscle, cardiac muscle, air). The model was implanted with planar biventricular epicardial leads (RA-lead: 9.4 cm length; RV lead: 11.7 cm length) connected to the cardiac muscle. The leads were modeled as a 1.5 mm perfect conductor (PEC) surrounded by a 2 mm insulator and connected to a pulse generator placed abdominally (as is common in pediatric patients). The pediatric model was placed in an MRI birdcage with the thoracic region placed at isocenter. The birdcage consisted of a 16-rung high-pass birdcage coil driven in quadrature to generate a circularly polarized excitation. The tuning capacitance was estimated and adjusted until the unloaded coil system was tuned to 64 MHz (31 pF) to simulate a 1.5 T MRI system. The input power was adjusted to produce a B1+RMS of 2.4 μT.

A total of 11 unique patient positions were analyzed and the 1-gram SAR_{local} was averaged on a 2 mm spherical radius around the RA and RV lead-tips. The positions analyzed included a combination of patient orientation with left-right positional shifts and lateral rotations within the scanner. All positions are in the image coordinate system. SAR_{local} was compared with respect to the *reference position* (Head first, supine, center). (Figure 1-A).

A. Patient Orientation

All the analyzed positions were performed on a head first orientation and then repeated on a feet orientation.

B. Left-Right Position

Simulations were performed for a supine head first and feet orientation and compared to left (-7 cm from isocenter) and right (+7 cm from isocenter) patient position shifts relative to isocenter. SAR_{local} was calculated for each position (Fig. 1-B).

C. Lateral Rotation

SAR_{local} was also calculated for both the head first and a feet orientation when the pediatric model was rotated laterally

Daniel B. Ennis Author is with the Department of Radiology, Stanford University, Stanford, CA 94305. (phone: +1-650-721-4641; e-mail: dbe@stanford.edu).
Jessica A. Martinez Author is with the Department of Radiology, Stanford University, Stanford, CA 94305. (e-mail: jmtz@stanford.edu).
Tyler E. Cork Author is with the Department of Radiology, Stanford University, Stanford, CA 94305. (e-mail: tecork@stanford.edu).
Henry E. Chubb Author is with the Department of Radiology, Stanford University, Stanford, CA 94305. (e-mail: mhchubb@stanford.edu).
Shreyas Vasanawala Author is with the Department of Radiology, Stanford University, Stanford, CA 94305. (e-mail: vasanawala@stanford.edu).

from a supine position (Fig. 1-B). The model was rotated clockwise and SAR_{local} was measured for three angles relative to the transverse plane (30°, 60°, 90°).

D. Paired SAR_{local} Analysis

The magnitude of SAR_{local} is expected to be greater for one CIED lead compared to the other lead, therefore a weighted average SAR_{local} ($wSAR_{local}$) was used to compare SAR_{local} differences for all the analyzed positions. The relative weights for the RA and RV were calculated following a convex combination [7] by adding the RA and RV SAR_{local} values and dividing by the individual lead value at the reference position.

In addition, the SAR_{local} percentage increase for each analyzed positions with respect to the reference position was calculated. Herein, the percentage increase was separated into three groups to categorize if the SAR_{local} resulted in non-substantial (≤33%), moderate (33%> and ≤66%), or substantial (>66%) percentage increase.

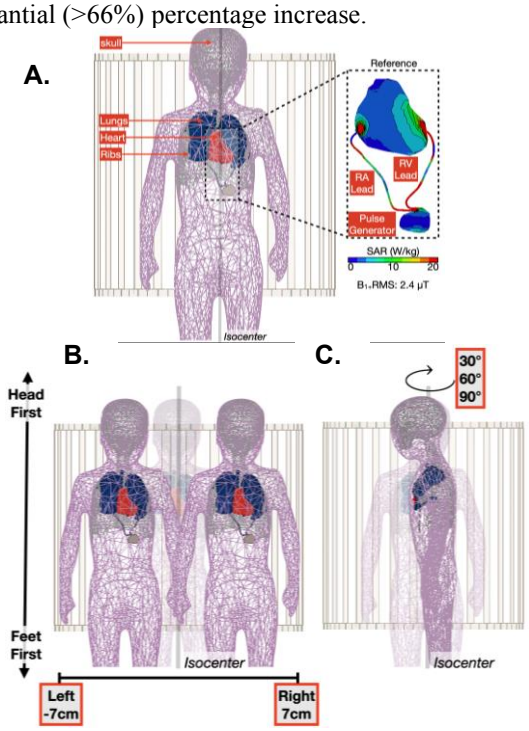

Figure 1. (A) Pediatric model setup and reference position for a thoracic exam. The model consisted of five compartments including heart muscle connected to an abdominal biventricular epicardial CIED. SAR_{local} was estimated for different patient positions and compared to the reference position with a B_{1+}RMS RF exposure of 2.4µT for a **(B)** left-right positional shift and **(C)** 30°/60°/90° lateral rotations.

III. Results

SAR_{local} values for the 11 positions were compared to the reference position. For the reference position, the greatest SAR_{local} values were observed for the RV lead compared to the RA lead (RV lead: 2196 W/kg; RA lead: 583 W/kg).

A. Left-Right Position

The RA and RV lead SAR_{local} for the left/right positional shifts and both patient orientations are shown in Figure 2. For the RA lead (Figure 2-A), the SAR_{local} was only mitigated for the right positional shift in a head first orientation (537 W/kg vs. 583 W/kg). For the RV lead (figure 2-B), the right positional shift resulted in a greater SAR_{local} for the RV lead (2458 W/kg vs. 2196 W/kg). Nevertheless, SAR_{local} for the RV lead was reduced for the left-most positional shift in a head first orientation and for the left-most and right-most positional shifts in a feet orientation.

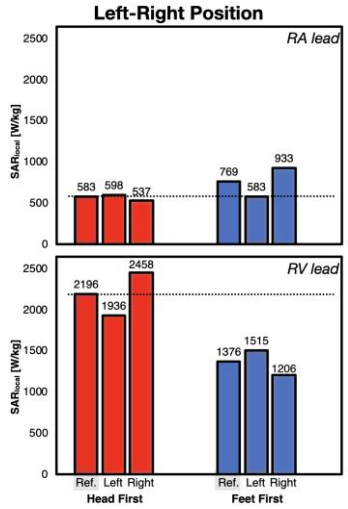

Figure 2. SAR_{local} values for the RA lead **(A)** and RV lead **(B)** with to the left-right (transverse) positional shifts and patient orientation (head first: red ; feet: blue). Dashed line highlights SAR_{local} reference value.

B. Lateral Rotation

The SAR_{local} for the RA and RV lead for each lateral rotation and both patient orientations are shown in Figure 3. For the RA lead (Figure 3-A), the SAR_{local} was reduced for the feet orientation when rotated 30º and 60º (30º: 419 W/kg, 60º: 461 W/kg vs. Ref: 583 W/kg). For the RV lead (Figure 3-B), all rotations resulted in lower SAR_{local} compared to the reference position. The lowest SAR_{local} for the RV lead was observed for the 60º rotation in a head first orientation (990 W/kg vs. Ref:2196 W/kg).

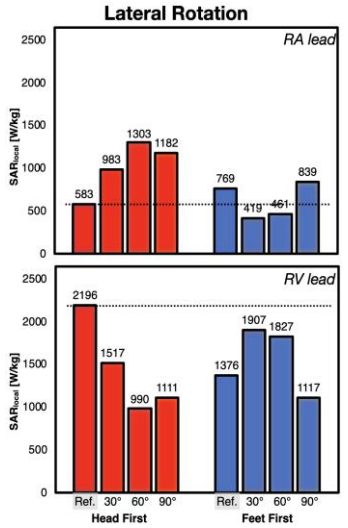

Figure 3. SAR_{local} values for the RA lead **(A)** and RV lead **(B)**. with respect of the lateral rotation and patient orientation (Head first: red; feet first: blue). Dashed line highlights SAR_{local} reference value.

C. *Paired SAR_{local} Analysis*

The $wSAR_{local}$ is provided in Table 1. The relative weights for the RV and RA leads in the reference position were 0.8 and 0.2 respectively. $wSAR_{local}$ was reduced for all analyzed positions except for the head first rightward positional shift. The minimum $wSAR_{local}$ was observed for the head first lateral rotation of 60º. Overall, all the patient positions using a feet orientation resulted in lower $wSAR_{local}$ compared to the reference position.

TABLE 1. Weighted average SAR_{local} ($wSAR_{local}$; RA weight: 0.2; RV weight: 0.8) for the analyzed positions. Red cell corresponds to the location in which $wSAR_{local}$ was greater with respect to the reference position.

Weighted Average SAR_{local} [W/kg]

	Ref.	30º	60º	90º	Left	Right
Head First	**1857**	1405	1056	1126	1655	2055
Feet First	1248	1595	1541	1059	1319	1149

Table 2 reports the SAR_{local} percentage change for the analyzed positions relative to the reference position. SAR_{local} for both the RA and RV resulted in different values with respect to position. Therefore, patient positions in which the SAR_{local} was reduced for the RV lead, did not necessarily result in lower SAR_{local} for the RA lead. Nevertheless, SAR_{local} for the RA lead was reduced for 3 of the 11 analyzed positions and 10 of the 11 positions for the RV lead.

Table 2 also indicates that 6 out of the 11 positions can result in SAR_{local} mitigation: two of these positions were in a head first orientation (left and right) and four in a feet first orientation (reference, 30º,60º and left). Nevertheless, the right head first position also showed an increase of the SARw, therefore SAR_{local} was not considered mitigated. From this cohort, three positions resulted in a non-substantial SAR_{local} increase of ≤33%, corresponding to the head first 30º and the feet 60º and leftward positional shifts will result in SAR_{local} percentage decrease compared to the reference position (Figure 4).

TABLE 2. SAR_{local} percentage change values with respect to the reference position. Non-substantial percentage increases are highlighted in green. Head first right positional shifts resulted in greater $wSAR_{local}$ thus SAR_{local} was not considered reduced (dashed green). Dark green highlights the positions in which a percentage decrease was observed.

		SAR_{local} Percentage Change [%]					
		Ref.	**30**	**60**	**90**	**Left**	**Right**
Head first	*RV*	**REF**	-31	-55	-49	-12	12
	RA	**REF**	69	124	103	3	-8
Feet First	*RV*	-37	-13	-17	-49	-31	-45
	RA	32	-28	-21	44	0	60

SAR_{local} Percentage Decrease ≤0%
Non-Substantial SAR_{local} Percentage Increase

IV. Discussion

In this work, pediatric patient positioning within the MRI scanner was investigated as a strategy for mitigating lead-tip heating. Lead-tip SAR_{local} was analyzed *in silico* in a pediatric model with a biventricular epicardial single-plane CIED for a range of practical patient orientations combined with left-right positional shifts and lateral rotations. The results suggest that switching pediatric patient positioning can be used as a simple technique to mitigate RF-induced heating. The weighted average SAR_{local} for the two leads suggests that SAR_{local} can be reduced for all the positions except for the right-most displacement in a head first orientation. This is consistent with the fact that the RF E-field is spatially asymmetric [8]; being greater in the left-anterior side area of the supine patient. Because SAR_{local} is proportional to the square of the RF E-Field, the SAR_{local} will increase when the magnitude of the RF E-field increases. For the CIED model used in this work, the RV lead falls in a greater E-field region, thus, exhibits greater SAR_{local} values compared to the RA lead. Therefore lead-tip heating and tissue damage may be greater for the RV lead. Nonetheless, SAR_{local} values for both RA and RV have simultaneously decreased relative to the reference position for three positions in a feet orientation following either a leftward positional shift or a lateral rotation between 30° and 60º.

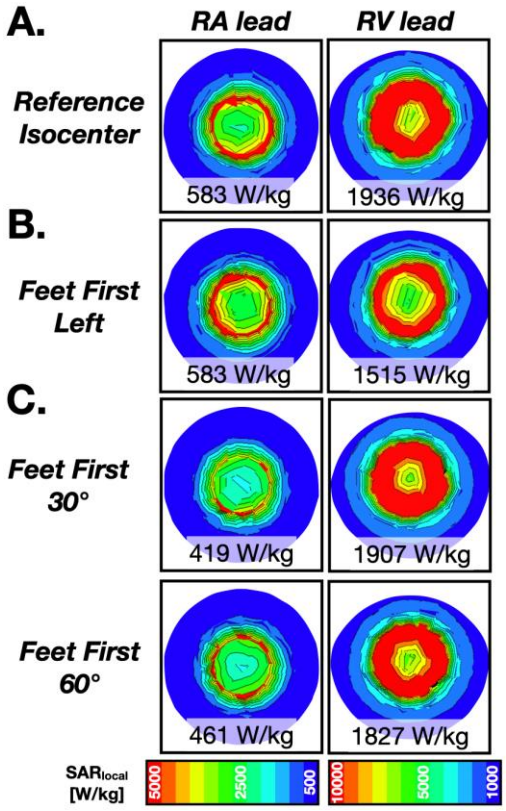

Figure 4. SAR_{local} maps and 1-gram average SAR_{local} values for a 2mm spherical volume around the RA and RV leads for **(A)** the reference position, **(B)** left/right displacement and **(C)** lateral rotations. The maps correspond to the positions in which the RA and RV lead SAR_{local} values were simultaneously reduced. **Note**: SAR_{local} colormaps between RA and RV lead have different limits.

The need to find methods to allow MRI exams for pediatric patients with CIEDs arises due to general contraindication for MRI exams due to the presence of CIEDs with epicardial leads, which may present excessive lead-tip heating. Most of the RF-induced heating studies have been designed for the

adult population, very few analyses have been performed to meet the needs of the pediatric population with implanted CIEDs. Hence, MR clinics lack mitigation strategies designed for the pediatric population. The modification of the patient positioning within the scanner works as a mitigation technique mostly because the incident E-field is modified which results in a reduction of SAR_{local} values at the lead-tips [9], [10]. Similar results have been found at 1.5T on the adult population when switching from a head first to a feet orientation [11], by rotation the position of the excitation ports within the scanner coil [12], or a variety of body regions or several patient rotations for head first examinations [13]. In general, placing a patient following a standard reference position (head first, isocenter) is only preferred since it is the most common position. Nonetheless, pediatric patients present more degree of freedom regarding patient positioning within the scanner considering the clinical standard MRI bore diameter (60-70 cm) and the median half chest-circumference for middle childhood pediatric patients (6-12 years old ~ 33 cm) [14]. Hence, modifying patient position is an inexpensive heating mitigation strategy for pediatric MRI examinations without affecting image quality.

The results presented here have some limitations. Firstly, the studies presented were performed for a planar biventricular epicardial lead path. Previous studies have demonstrated that lead-tip heating and SAR_{local} will be affected by the specific lead-path. Herein, we opted to analyze a planar lead path, to ensure worst-case SAR_{local} as suggested in the RF heating safety guidelines [15], [16]. To translate these results into clinical practice, it is necessary to analyze the relationship between patient position and anatomically realistic lead-paths.

Secondly, previous analyses have highlighted that the landmark or body region under examination for adult patients with CIEDS will also affect lead-tip heating. Maximum lead-tip heating values are expected for thoracic examinations (i.e. CIED close to isocenter); whereas minimum lead-tip heating is observed when the CIED is distant from isocenter (brain or lower extremity exams). Herein, only thoracic examinations were examined. However, pediatric patients are typically much shorter than adult patients and the patient position shifts relative to isocenter are much smaller. Nevertheless, additional simulations could be done to identify that pediatric patient positioning relative to isocenter can also mitigate SAR_{local} and lead-tip heating across all landmarks.

Lastly, the SAR_{local} analysis provides insight into the heating behavior at the CIED lead-tip, but it is necessary to perform *in vitro* thermometry and calorimetry analysis during RF exposure to CIEDs in the scanner to confirm that patient positioning is a robust method to mitigate lead-tip heating and confer better patient safety.

V. Conclusion

Computer simulations demonstrate that modifying pediatric patient positioning can mitigate CIED lead-tip heating. The positions that best reduce lead-tip heating include switching to a feet orientation, a leftward positional shift, or a lateral rotation. Future work needs to analyze different lead paths, landmarks, and to perform *in vitro* testing.

References

[1] H. R. Singh, A. S. Batra, and S. Balaji, "Pacing in children," Ann. Pediatr. Cardiol., vol. 6, no. 1, pp. 46–51, 2013, doi: 10.4103/0974-2069.107234.

[2] M. Bireley et al., "Cardiac Magnetic Resonance Imaging (MRI) in Children is Safe with Most Pacemaker Systems, Including Those with Epicardial Leads," Pediatr. Cardiol., vol. 41, no. 4, pp. 801–808, Apr. 2020, doi: 10.1007/s00246-020-02316-z.

[3] G. K. Lui et al., "Diagnosis and Management of Noncardiac Complications in Adults With Congenital Heart Disease: A Scientific Statement From the American Heart Association," Circulation, vol. 136, no. 20, pp. e348–e392, Nov. 2017, doi: 10.1161/CIR.0000000000000535.

[4] J. Rekawek et al., "Risk factors for cardiac arrhythmias in children with congenital heart disease after surgical intervention in the early postoperative period," J. Thorac. Cardiovasc. Surg., vol. 133, no. 4, pp. 900–904, Apr. 2007, doi: 10.1016/j.jtcvs.2006.12.011.

[5] J. H. Indik et al., "2017 HRS expert consensus statement on magnetic resonance imaging and radiation exposure in patients with cardiovascular implantable electronic devices," Heart Rhythm, vol. 14, no. 7, pp. e97–e153, Jul. 2017, doi: 10.1016/j.hrthm.2017.04.025.

[6] J. A. Martinez and D. B. Ennis, "MRI of Patients with Cardiac Implantable Electronic Devices," Curr. Cardiovasc. Imaging Rep., vol. 12, no. 7, p. 27, May 2019, doi: 10.1007/s12410-019-9502-8.

[7] Convex Analysis. 1997. Accessed: May 03, 2021. [Online]. Available: https://press.princeton.edu/books/paperback/9780691015866/convex-analysis

[8] P. Nordbeck et al., "Spatial distribution of RF-induced E-fields and implant heating in MRI," Magn. Reson. Med., vol. 60, no. 2, pp. 312–319, Aug. 2008, doi: 10.1002/mrm.21475.

[9] P. Nordbeck et al., "Spatial distribution of RF-induced E-fields and implant heating in MRI," Magn. Reson. Med., vol. 60, no. 2, pp. 312–319, Aug. 2008, doi: 10.1002/mrm.21475.

[10] P. Nordbeck et al., "Measuring RF-induced currents inside implants: Impact of device configuration on MRI safety of cardiac pacemaker leads," Magn. Reson. Med., vol. 61, no. 3, pp. 570–578, 2009, doi: https://doi.org/10.1002/mrm.21881.

[11] J. A. Martinez, P. Serano, and D. B. Ennis, "Patient Orientation Affects Lead-Tip Heating of Cardiac Active Implantable Medical Devices during MRI," Radiol. Cardiothorac. Imaging, vol. 1, no. 3, p. e190006, Aug. 2019, doi: 10.1148/ryct.2019190006.

[12] E. Lucano et al., "A numerical investigation on the effect of RF coil feed variability on global and local electromagnetic field exposure in human body models at 64 MHz," Magn. Reson. Med., vol. 79, no. 2, pp. 1135–1144, 2018, doi: 10.1002/mrm.26703.

[13] L. Golestanirad et al., "Reconfigurable MRI coil technology can substantially reduce RF heating of deep brain stimulation implants: First in-vitro study of RF heating reduction in bilateral DBS leads at 1.5 T," PLoS ONE, vol. 14, no. 8, Aug. 2019, doi: 10.1371/journal.pone.0220043.

[14] C. Li, E. S. Ford, A. H. Mokdad, and S. Cook, "Recent Trends in Waist Circumference and Waist-Height Ratio Among US Children and Adolescents," Pediatrics, vol. 118, no. 5, pp. e1390–e1398, Nov. 2006, doi: 10.1542/peds.2006-1062.

[15] ASTM International, "F2182-19e2 Standard Test Method for Measurement of Radio Frequency Induced Heating On or Near Passive Implants During Magnetic Resonance Imaging," ASTM International, 2019. doi: 10.1520/F2182-11A.

[16] "ISO/TS 10974:2012 - Assessment of the safety of magnetic resonance imaging for patients with an active implantable medical device." https://www.iso.org/standard/46462.html (accessed May 08, 2018).